Ther Adv Neurol Disord
2020, Vol. 13: 1–10
DOI: 10.1177/1756286420925679

Prediction of motor recovery using indirect connectivity in a lesion network after ischemic stroke

Jungsoo Lee, Eunhee Park, Ahee Lee, Won Hyuk Chang, Dae-Shik Kim and Yun-Hee Kim

Abstract

Background: Recovery prediction can assist in the planning for impairment-focused rehabilitation after a stroke. This study investigated a new prediction model based on a lesion network analysis. To predict the potential for recovery, we focused on the next link-step connectivity of the direct neighbors of a lesion.

Methods: We hypothesized that this connectivity would contribute to recovery after stroke onset. Each lesion in a patient who had suffered a stroke was transferred to a healthy subject. First link-step connectivity was identified by observing voxels functionally connected to each lesion. Next (second) link-step connectivity of the first link-step connectivity was extracted by calculating statistical dependencies between time courses of regions not directly connected to a lesion and regions identified as first link-step connectivity. Lesion impact on second link-step connectivity was quantified by comparing the lesion network and reference network.

Results: The lower the impact of a lesion was on second link-step connectivity in the brain network, the better the improvement in motor function during recovery. A prediction model containing a proposed predictor, initial motor function, age, and lesion volume was established. A multivariate analysis revealed that this model accurately predicted recovery at 3 months poststroke ($R^2 = 0.788$; cross-validation, $R^2 = 0.746$, $RMSE = 13.15$).

Conclusion: This model can potentially be used in clinical practice to develop individually tailored rehabilitation programs for patients suffering from motor impairments after stroke.

Keywords: lesion network, motor function, motor recovery, prediction model, stroke

Received: 1 January 2020; revised manuscript accepted: 20 April 2020.

Correspondence to:
Yun-Hee Kim
Department of Physical and Rehabilitation Medicine, Center for Prevention and Rehabilitation, Heart Vascular Stroke Institute, Samsung Medical Center, Sungkyunkwan University School of Medicine, Department of Health Sciences and Technology, Department of Medical Device Management & Research, Department of Digital Health, SAIHST, Sungkyunkwan University, 81 Irwon-ro, Gangnam-gu, Seoul 06351, Republic of Korea
yunkim@skku.edu, **yun1225.kim@samsung.com**

Jungsoo Lee
Won Hyuk Chang
Department of Physical and Rehabilitation Medicine, Samsung Medical Center, Sungkyunkwan University School of Medicine, Seoul, Republic of Korea

Eunhee Park
Department of Physical and Rehabilitation Medicine, Kyungpook National University Medical Center, Daegu, Republic of Korea

Ahee Lee
Department of Health Sciences and Technology, Department of Medical Device Management & Research, Department of Digital Health, SAIHST, Sungkyunkwan University, Seoul, Republic of Korea

Dae-Shik Kim
School of Electrical Engineering, Korea Advanced Institute of Science and Technology, Daejeon, Republic of Korea

Introduction

Stroke is the leading cause of acquired disabilities in adults.[1] Stroke-related impairments cause drastic reductions in patients' daily living activities and quality of life. To regain independence and quality of life after stroke, effective rehabilitation planning is essential. Recovery prediction can help clinicians design individually tailored rehabilitation plans, including realistic discharge planning and appropriate allocation of time and resources. In addition, it allows patients to set realistic goals.[2]

Neuroimaging-based brain connectivity analyses are already used in recovery prediction, and several predictors have been identified.[3–7] Neurologic research has emphasized that the effects of neurological disorders are exerted over an entire network because the brain is organized in networks of connections among many neurons.[8–10] Damage caused by stroke can diffuse through the brain networks and influence the function of distant brain regions even when the damage to the brain structure is a focal lesion.[9,11] Therefore, using a brain connectivity analysis for recovery prediction is an appropriate approach. However, prediction remains difficult because of inter-individual variability.

Previous clinical studies have used various predictive markers. Among them, initial motor function is the most representative.[2,12,13] However, it has

limitations in predicting motor recovery in patients with severe stroke.[13] Furthermore, for clinical purposes, an accurate prediction model beyond initial motor function itself is needed. Our aim in this study was to use magnetic resonance imaging (MRI) data and initial motor function in a brain connectivity analysis to propose a new predictor that can accurately predict recovery from stroke.

Previous studies have demonstrated widespread remote changes in connectivity in regions in both hemispheres as the result of a focal lesion.[8,14,15] Also, motor learning after stroke is performed by widespread networks in the whole brain, without the need for a motor-related central region, and many regions in widespread networks compensate for learning success.[16] In this respect, an investigation of the overall connectivity in the whole brain and the indirect connectivity of the damaged area, beyond the direct connectivity of the damaged area, might be important for understanding recovery after stroke.

The second link-step connectivity of a lesion network (the next link-step beyond a lesion's direct connectivity) was obtained from resting-state functional MRI (fMRI) and investigated using the following considerations: (a) second link-step connectivity is likely to be highly affected by a lesion because connectivity is adjacently connected to a lesion when considering the spread of damage throughout the entire network; (b) the connectivity forms a wider brain network and broadly covers more brain regions than first link-step connectivity in terms of information spreading within a network structure. Therefore, by quantifying second link-step connectivity, the impact of the focal lesion on the whole brain network can be assessed according to points (a) and (b). Furthermore, this connectivity is expected to actively contribute to recovery after stroke onset because it does not suffer actual physical damage from the focal lesion. During the recovery period, a lesion with a low impact on connectivity enables cost-effective reorganization to allow recovery across the whole brain network, so second link-step connectivity might indicate the potential for functional recovery. Therefore, we hypothesized that patients whose lesions had a low impact on second link-step connectivity would be more likely to recover from stroke damage, as reflected by better motor recovery, than patients whose lesions had high impacts on second link-step connectivity.

Materials and methods

Participants and experimental design

A total of 64 patients who had suffered ischemic stroke (36 men and 28 women, aged 57.9 ± 12.6 years) underwent MRI data acquisition 2 weeks after stroke onset (T1), and their motor function was measured on the same day as MRI data acquisition. At 3 months after stroke onset (T2), motor function was measured again to assess functional improvement. The Fugl–Meyer assessment (FMA)[17] score was used as a measurement of motor function. The T1 FMA score was also used as a measure of initial motor function (baseline). These subjects were collected from the stroke database held by the Department of Physical and Rehabilitation Medicine at Samsung Medical Center, which has been collecting MRI data from patients who had suffered strokes and healthy subjects since 2007. Inclusion criteria were first-onset unilateral ischemic stroke and age 19 years or older at the time of stroke onset. Patients were excluded if they exhibited any clinically significant or unstable medical conditions, any neuropsychiatric comorbidity other than stroke, or any contraindication to MRI. The clinical information of participants is summarized in Table 1 and Supplemental Table 1. Resting-state fMRI data from 64 healthy subjects (26 men and 38 women, aged 50.0 ± 16.5 years) who reported no history of psychiatric or neurological problems were also used in this study. This retrospective study was performed in accordance with relevant guidelines and the regulations of the Declaration of Helsinki. Ethical approval was obtained from the Institutional Review Board (IRB) of Samsung Medical Center, Seoul, Republic of Korea. We received an exemption from informed consent from the IRB because we used only previously collected data and did not exceed minimal risk.

Data acquisition

Participants were instructed to keep their eyes closed and remain motionless during the resting-state fMRI scan. The fMRI data were acquired using a Philips ACHIEVA® MR scanner (Philips Medical Systems, Best, The Netherlands) operating at 3 T. During each session, 100 whole-brain images were collected using a T2*-weighted, gradient echo-planar imaging sequence with the following metrics: 35 axial slices, slice thickness = 4 mm, no gap,

Table 1. Patient demographics.

Age (years)	
Mean ± SD	57.9 ± 12.6
Sex (*n*)	
Male	36
Female	28
Side of lesion (*n*)	
Right	33
Left	31
Bilateral	0
Location of lesion (*n*)	
Supratentorial	45
Infratentorial	19
Type of stroke (*n*)	
Hemorrhagic	0
Ischemic	64
Initial severity (*n*)	
Mild and moderate (FMA >55)	19
Severe (FMA ⩽55)	45
Time poststroke (days)	
T1, Mean ± SD	14.8 ± 6.9
T2, Mean ± SD	97.4 ± 11.7
FMA scores	
T1, Mean ± SD	43.5 ± 23.3
T2, Mean ± SD	67.5 ± 25.9

FMA, Fugl–Meyer Assessment; SD, standard deviation; T1, 2 weeks poststroke; T2, 3 months poststroke.

matrix size = 128 × 128, repetition time = 3000 ms, echo time = 35 ms, flip angle = 90°, and field of view = 220 × 220 mm. T1-weighted images were acquired with the following settings: 124 axial slices, slice thickness = 1.6 mm, no gap, matrix size = 512 × 512, repetition time = 13.9 ms, echo time = 6.89 ms, flip angle = 8°, and field of view = 240 × 240 mm for lesion segmentation and atlas transformation.

Data processing

Preprocessing was performed using the SPM8 package (Welcome Trust Centre for Neuroimaging, University College London, London, UK). Functional images were processed as follows: (a) slice timing correction; (b) spatial realignment for head motion correction; (c) spatial normalization into the Montreal Neurological Institute (MNI) atlas space resampling to 2-mm isotropic voxels. Spatial smoothing of the normalized images was performed using a 6-mm full-width half-maximum Gaussian kernel. For the connectivity analysis, several nuisance sources were removed by linear regression of 22 nuisance parameters. Parameters were obtained from six head motion parameters and six first-order temporal derivatives of the motion parameters. Each of the five parameters was obtained from a principal component analysis of the temporal components of white matter and ventricle signals as nuisance regressors for effective noise correction.[18] Band-pass filtering between 0.009 and 0.08 Hz was performed to remove constant offsets and linear trends. Nuisance regression and band-pass filtering were processed using MATLAB (MathWorks, Natick, MA, USA).

Connectivity was obtained by calculating the statistical dependencies between time courses using Pearson's correlation coefficients. We examined positive correlation coefficients in this study. A voxel-wise connectivity analysis (seed-based approach) was used to extract the first link-step connectivity. The connectivity map had a threshold of $p < 0.00005$ (uncorrected).[19] A region-wise connectivity analysis was used to extract second link-step connectivity. An automated anatomical labeling (AAL) template[20] was used for the region-wise connectivity analysis. The AAL template was segmented into 116 regions (90 regions in the cerebrum and 26 regions in the cerebellum) covering the whole brain. We averaged nine regions in the left and right cerebellum and eight regions in the vermis. The brainstem region was added by drawing it manually on the AAL atlas. The resulting modified AAL atlas, which contained 94 regions, was co-registered to the normalized fMRI data space using SPM8 and then analyzed.

Each patient lesion was segmented on a T1-weighted structural image with reference to apparent hyper-intensities on a diffusion-weighted image that was acquired at the patient's first neurology appointment. One medical doctor manually drew the lesion maps of all patients using MRIcro lesion

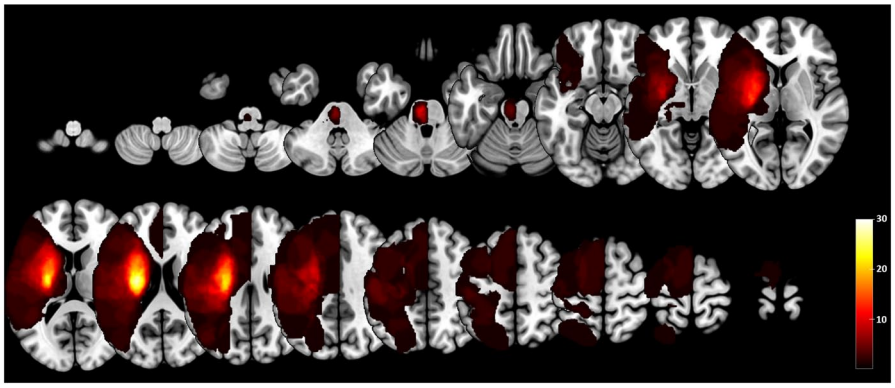

Figure 1. Lesion maps. All masks of stroke lesions were flipped to the right hemisphere. The colored bar indicates the number of patients.

mapping software (https://www.mccauslandcenter.sc.edu/crnl/). Each lesion was normalized into the standard MNI space. The results were visualized using the xjView toolbox (http://www.alivelearn.net/xjview) (Figure 1). The lesion side of the map was flipped to the right side for visualization.

Second link-step functional connectivity from lesions

Recently, a lesion network mapping method has been used to investigate the expanding localization of symptoms from heterogeneous lesions.[19,21] That method is based on lesion-seeded, resting-state, functional connectivity. We based our extraction of a lesion's second link-step connectivity on that lesion network mapping method. Our framework involved seven steps (Figure 2). (Step 1) The lesion image of a patient and the resting-state fMRI of a healthy subject were normalized into the standard MNI space. The normalized lesion was used as the first seed region in the seed-based approach. (Step 2) A seed-voxel-based approach was performed using a mean time course of the lesion volume in resting-state fMRI of a healthy subject (first link-step, voxel-wise connectivity, $p < 0.00005$). Extracting that first link-step connectivity of a lesion is similar to the previously published lesion network mapping method.[19] (Step 3) The second seed was the volume of all the lesion-seeded connected voxels (the first link-step connectivity of the lesion) in a region of the modified AAL atlas. Therefore, multiple second seeds were found because the first link-step connectivity covered multiple regions. (Step 4) The connectivity was calculated between the mean time course of the second seed and the mean time courses of all other AAL atlas regions except for the lesion-seeded connected voxels (second link-step, region-wise connectivity, $p < 0.01$). (Step 5) Step 4, region-wise connectivity, was repeated for each second seed region, and an adjacency matrix was constructed by inserting the correlation values in rows corresponding to the seed regions. (Step 6) The asymmetric adjacency matrix obtained from Step 5 was then made symmetric by adding the transpose matrix. For example, say that two regions in the modified AAL atlas (regions 1 and 2) contain lesion-seeded connected voxels. The second seed in region 1 consists of all the lesion-seeded connected voxels in region 1, and the connectivity ($W_{(1,2)}$) is calculated between the mean time course of the second seed in region 1 and the mean time course of all the voxels in region 2 except the lesion-seeded connected voxels. Meanwhile, the second seed in region 2 contains the lesion-seeded connected voxels in region 2, and the connectivity ($W_{(2,1)}$) is calculated between the mean time course of the second seed in region 2 and the mean time course of all the voxels in region 1 except the lesion-seeded connected voxels. We transformed the asymmetric matrix into a symmetric matrix by adding the transpose matrix ($W_{(1,2)} + W_{(2,1)}$). If two regions include second seeds (lesion-seeded connected voxels), we wanted to reflect an aggravated effect between regions 1 and 2 to distinguish that situation from one in which only a single region has a second seed ($W_{(1,2)}$ or $W_{(2,1)}$) to clarify the contrast of lesion impact. (Step 7) The adjacency

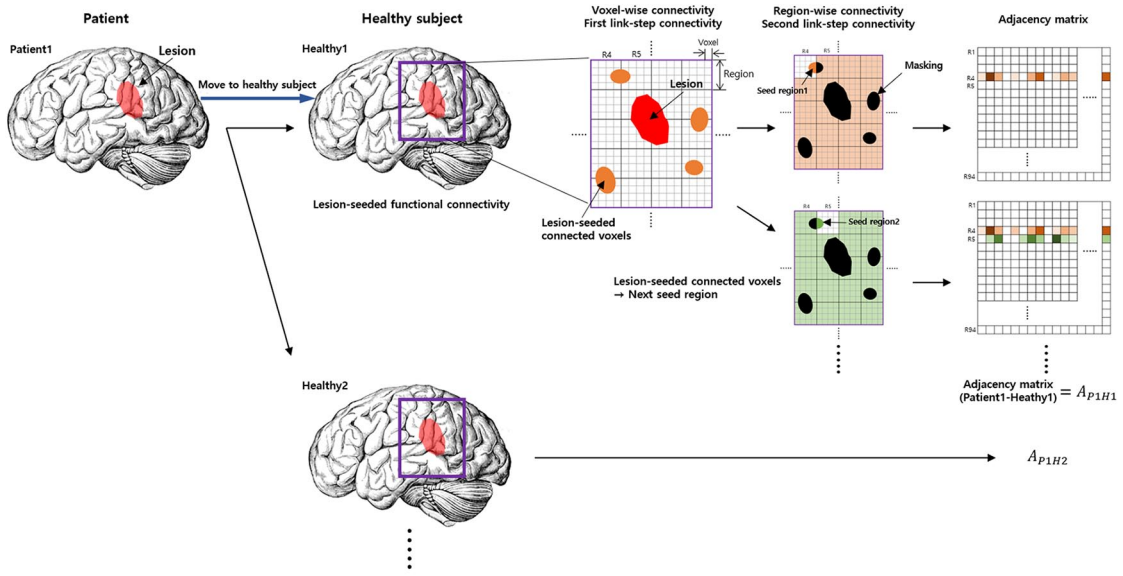

Figure 2. Framework to extract the second link-step connectivity of a lesion.

matrices corresponding to a lesion were repeatedly obtained from all healthy subjects ($A_{P1H1}, A_{P1H2}, A_{P1H3}, ...$) by following Step (1) through Step (6), and then all the matrices were averaged. The averaged matrix represents the second link-step connectivity of one lesion. Therefore, the second link-step connectivity matrix of a patient lesion (A_{P1}) was defined as follows:

$$A_{P1} = \frac{\sum_{i=1}^{n} A_{P1Hi}}{n}$$

where A_{P1Hi} is the second link-step connectivity matrix of the *i-th* healthy subject, and n is the number of healthy subjects. All matrices $A_{P1} - A_{P64}$ are illustrated in Supplemental Figure 1.

We quantitatively measured the impact of a lesion on the brain network by counting the number of unconnected and weaker connections compared with the reference connectivity matrix (ref_A) in the second link-step connectivity matrix (A matrix). The number of connections is our predictor in the study. The ref_A was obtained by averaging the modified AAL connectivity matrices of all healthy subjects. The connectivity matrix does not mask any lesion area, and the lesion-seeded connected voxels and intrinsic connectivity matrix are extracted.

$$C_{ij} = \frac{A_{ij}}{ref\_A_{ij}}$$

$$C_{ij} = \begin{cases} 1, & if\ C_{ij} < 1\ and\ i \neq j \\ 0, & otherwise \end{cases}$$

$$Predictor = \sum_{i=1}^{m}\sum_{j=1}^{m} C_{ij}$$

where A_{ij} is an element of the second link-step connectivity matrix of one patient, ref_A_{ij} is an element of the reference connectivity matrix, m is the number of regions, and C_{ij} is illustrated in Supplemental Figure 2. In this study, a connection with less than the reference connection strength was defined as a connection that was weakly impacted by the lesion. A connection with no strength was defined as a connection that was not indirectly impacted by the lesion. Therefore, our proposed predictor corresponds to the number of connections with weak and no lesion impacts.

Statistical analysis

We used linear regression to identify the relationship between the improvement of motor function and the proposed predictor. A multiple regression was also used to establish the proposed prediction model using the proposed predictor and patient

characteristics. Leave-one-out cross-validation (LOOCV) and k-fold cross-validation were performed to assess the performance of our proposed prediction model. These statistics were derived using the statistics toolbox of MATLAB R2014b.

Results

Univariate analysis

The second link-step connectivity of 64 lesions was extracted. The proposed predictor used the number of second link-step connections (the number of connections in the adjacency matrix in Supplemental Figure 2). A linear regression model was used to investigate the relationships between the proposed predictor and motor function recovery (ΔFMA = FMA (T2) – FMA (T1)) (Figure 3(a)). The predictor did correlate with motor function recovery (r=0.470, p=8.79e-05, R^2 = 0.221). We also divided patients into groups based on whether their lesion was supratentorial or infratentorial, and again investigated the relationship between our predictor and improvements in motor function (Figure 3(b) and (c)). Our predictor was highly significant for patients with supratentorial lesions but not for patients with infratentorial lesions (supratentorial lesions, r=0.588, p=2.15e-05, R^2 = 0.346; infratentorial lesions, r=0.295, p=0.2217, R^2 = 0.087). When assessing the relationship between the clinical characteristics of patients and motor function recovery, we found that age and lesion volume correlated with motor function recovery (age, r=0.335, p=0.0068, R^2 = 0.112; lesion volume, r=0.257, p=0.0403, R^2 = 0.066) (Supplemental Figure 3).

Multivariate analysis for supratentorial lesions

We investigated the combined model between both variables (predictor + baseline) using a multiple linear regression model. The combined model demonstrated high accuracy in predicting motor function after 3 months (FMA (T2)) (r=0.868, p=1.13e-14, R^2 = 0.753, root mean square error (RMSE) = 12.97) (Figure 3(d)). A multivariate analysis considering patient characteristics at baseline, age, and lesion volume as independent factors was performed. The best prediction model was *FMA (T2) ~ 1 + Predictor + Baseline + Age + log(Lesion volume)* (r=0.888, p=3.79e-16, R^2 = 0.788, *RMSE* = 12.01) (Figure 3(e)). In the multivariate analysis (Table 2), the proposed predictor remained significant and contributed significantly to the accuracy of the prediction.

A multivariate analysis of all variables except the proposed predictor was performed to investigate the proposed predictor's worth in predicting motor function. This model was *FMA (T2) ~ 1 + Baseline + Age + log(Lesion volume)* (r=0.824, p=3.14e-12, R^2 = 0.679, *RMSE* = 14.77). R^2 increased by more than 0.1 when our proposed predictor was added and RMSE decreased by more than 2.7. Our proposed predictor thus valuably enhanced the accuracy of the prediction. Furthermore, the proposed predictor was not correlated with other variables (lesion volume, p=0.8264; age, p=0.2004; baseline, p=0.7127).

Cross-validation

The LOOCV results are shown in Figure 3(f), which shows the relationship between the predicted FMA score obtained from the model and the actual FMA score obtained from the test data at 3 months poststroke. Those results verify the performance of our model (r=0.864, p=2.08e-14, R^2 = 0.746, *RMSE* = 13.15). A 9-fold cross-validation (5 test datasets, 40 training datasets) was also performed, and the mean performance (r=0.863, p=3.12e-14, R^2 = 0.744, *RMSE* = 13.19) obtained after 30 trials was similar to the LOOCV results.

Discussion

Second link-step connectivity as a recovery predictor

One of the main findings of this study was that the impact of a lesion on the second link-step connectivity is related to improvement in motor function during the recovery period. This is distinct from previous studies that focused on connections directly damaged by a lesion. Several recent studies have demonstrated widespread remote changes in connectivity in regions between both hemispheres due to a focal lesion.[8,14,15] Furthermore, Beckman *et al.* showed that a focal lesion impacted brain connectivity in diverse networks,[22] regardless of the location of the affected or unaffected side or the motor network.[8,14,23] The terms 'connectional' and 'connectomal diaschisis' have been coined recently.[11] Based on these studies, we hypothesized that measuring the impact of a focal

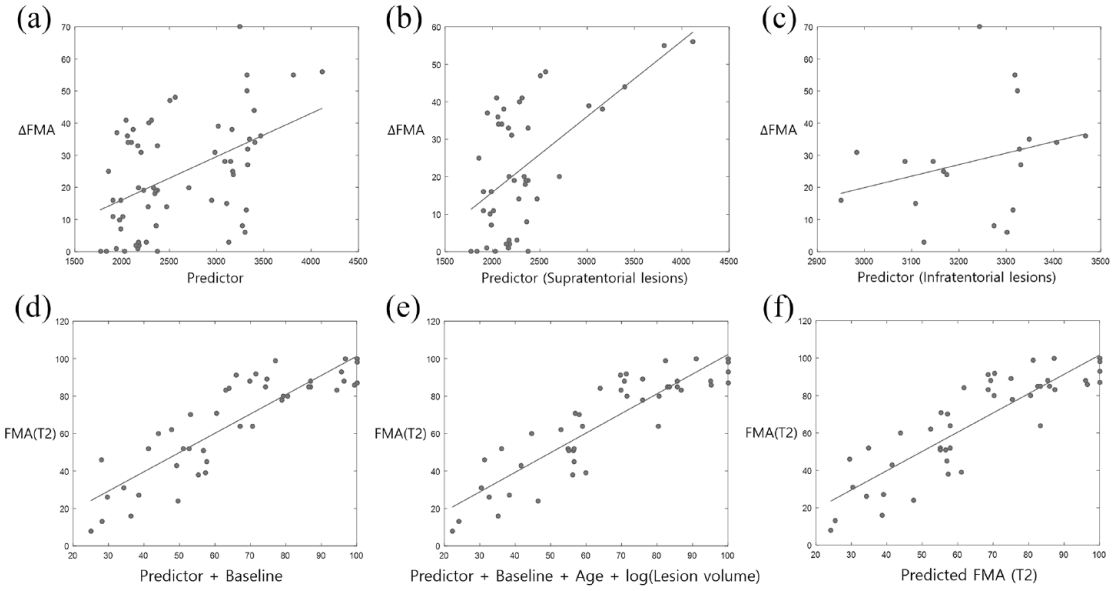

Figure 3. Relationships between variables (proposed predictor (a), proposed predictor for supratentorial lesions (b), and proposed predictor for infratentorial lesions (c)) and motor function recovery (ΔFMA) in univariate analysis (all lesions, $r = 0.470$, $p = 8.79e\text{-}05$, $R^2 = 0.221$; supratentorial lesions, $r = 0.588$, $p = 2.15e\text{-}05$, $R^2 = 0.346$; infratentorial lesions, $r = 0.295$, $p = 0.2217$, $R^2 = 0.087$). (d) Relationship between the combined model (baseline + proposed predictor) and motor function at 3 months poststroke (FMA (T2)) ($r = 0.868$, $p = 1.13e\text{-}14$, $R^2 = 0.753$). (e) Results from the multiple linear regression model [*FMA (T2) ~ 1 + Predictor + Baseline + Age + log(Lesion volume)*] ($r = 0.888$, $p = 3.79e\text{-}16$, $R^2 = 0.788$). (f) Validation results. Relationship between predicted motor function (predicted FMA (T2)) and actual motor function at 3 months poststroke (FMA (T2)) ($r = 0.864$, $p = 2.08e\text{-}14$, $R^2 = 0.746$, $RMSE = 13.15$).
FMA, Fugl–Meyer Assessment; RMSE, root-mean-square error; T2, 3 months poststroke.

Table 2. Multiple linear regression model.

FMA (T2) ~ 1 + Predictor + Baseline + Age + log(Lesion volume)				
Variable	**Estimate**	**SE**	***t* value**	***p* value**
Predictor	0.3408	0.076	4.46	6.42e-05
Baseline	0.8087	0.077	10.46	5.21e-13
Age	−0.1107	0.079	−1.40	0.1678
log(Lesion volume)	−0.1446	0.076	−1.90	0.0646

FMA, Fugl–Meyer Assessment; SE, standard error; T2, 3 months poststroke.

lesion on large-scale networks might be valuable for designing rehabilitation plans and determining prognosis. We demonstrated that the less the impact of a lesion on second link-step connectivity in a whole brain network, the better the improvement in motor function. In this study, age and lesion volume were also associated and negatively correlated with improved motor function, in agreement with previous studies.[24–27]

Recovery prediction using resting-state functional connectivity analysis

Resting-state functional connectivity (rs-FC) analysis has been used widely in neurologic research to investigate recovery patterns and to find recovery-related indicators. However, anatomical or diffusion tensor imaging (DTI) data analysis has primarily been used in recovery prediction studies.[28] These analyses are useful for

investigating the direct influences of a lesion location, size, or damaged motor pathways. In this study, we focused on indirectly damaged connectivity (second link-step connectivity) to predict functional recovery. rs-FC analysis is more flexible than anatomical or DTI analysis. In other words, rs-FC analysis has fewer technical limitations than the other two techniques, which is why we chose it to validate our hypothesis. Stroke lesions include white matter structures. Typically, fMRI analysis is applied to investigate neural signals in gray matter structures. Several recent studies have investigated fMRI signals in white matter structures.[29–33] In addition, convergence between anatomical connectivity obtained from DTI analysis and functional connectivity obtained from rs-FC analysis has been detected,[34] and novel analyses such as lesion network mapping using fMRI signals obtained from white matter structures have been applied to study neurological disorders.[19,21,34] We validated the importance of indirectly damaged connectivity and confirmed the potential of our method for predicting recovery using rs-FC analysis.

Advantages and limitations of the study

First link-step and second link-step connectivities from a lesion were obtained sequentially from healthy subjects. Many second link-step connectivity matrices from all healthy subjects were averaged to obtain the second link-step connectivity from each lesion. This improves the signal to noise ratio. We verified our model in a wide variety of initial impairment patients (from extremely severe to slightly severe patients). In a previous study, initial impairment showed relatively low prediction accuracy in patients with a severe initial deficit.[35] Our model demonstrated high predictive accuracy even though severe patients (FMA (T1) $\leqslant$55) who showed high variability in recovery composed a large proportion of our test population.

This study also had several limitations. First, the proposed predictor was less valuable for infratentorial lesions than supratentorial lesions. Our method mainly assessed the global effect of lesions in cortical regions, and the functional connectivity of the pons or medulla is sparse in cortical regions.[19,36] The brainstem regions also include physiological noise, such as cardiac and respiratory cycles, which should be removed through physiological monitoring.[37,38] As a result, the second link-step connectivity of infratentorial lesions in our study had relatively low strength and was indistinguishable among lesions (Supplemental Figure 4). Another limitation of this study is the period of recovery. In this study, FMA improvement scores from approximately 3 months after stroke onset were used to quantify motor function recovery. Additional motor function can be recovered after a longer period of time. However, according to previous studies, most spontaneous recovery occurs within the first 3 months after stroke onset.[39] Lastly, information related to the spatial topography of the second link-step connectivity is not provided. That information would provide insight for noninvasive brain stimulation protocols. Beyond the magnitude of the index, further study regarding that spatial topography is needed.

Conclusion

We measured lesion impacts on second link-step connectivity in the lesion network to develop a predictor of stroke recovery and proposed a prediction model to predict motor function 3 months poststroke. The model, including a proposed predictor, initial motor function, lesion volume, and age, demonstrated high accuracy for predicting motor function at 3 months poststroke. This model can potentially be used in clinical practice to develop individually tailored rehabilitation programs for patients suffering from motor impairments after stroke.

Funding

The authors disclosed receipt of the following financial support for the research, authorship, and/or publication of this article: This work was supported by a National Research Foundation of Korea (NRF) grant funded by the Korean government (NRF-2020R1A2C3010304, NRF-2020R1C1C1011688, NRF-2017M3A9G5083690).

Conflict of interest statement

The authors declare that there is no conflict of interest.

ORCID iD

Yun-Hee Kim https://orcid.org/0000-0001-6101-8851

Supplemental material

Supplemental material for this article is available online.

References

1. Go AS, Mozaffarian D, Roger VL, *et al*. Heart disease and stroke statistics-2014 update. *Circulation* 2014; 129: e28–e292.
2. Stinear C. Prediction of recovery of motor function after stroke. *Lancet Neurol* 2010; 9: 1228–1232.
3. Siegel JS, Ramsey LE, Snyder AZ, *et al*. Disruptions of network connectivity predict impairment in multiple behavioral domains after stroke. *Proc Natl Acad Sci USA* 2016; 113: E4367–E4376.
4. Kuceyeski A, Navi BB, Kamel H, *et al*. Structural connectome disruption at baseline predicts 6-months post-stroke outcome. *Hum Brain Mapp* 2016; 37: 2587–2601.
5. Jiang L, Xu H and Yu C. Brain connectivity plasticity in the motor network after ischemic stroke. *Neural Plast* 2013; 2013.
6. Burke Quinlan E, Dodakian L, See J, *et al*. Neural function, injury, and stroke subtype predict treatment gains after stroke. *Ann Neurol* 2015; 77: 132–145.
7. Lee J, Lee M, Kim D-S, *et al*. Functional reorganization and prediction of motor recovery after a stroke: a graph theoretical analysis of functional networks. *Restor Neurol Neurosci* 2015; 33: 785–793.
8. Carter AR, Astafiev SV, Lang CE, *et al*. Resting interhemispheric functional magnetic resonance imaging connectivity predicts performance after stroke. *Ann Neurol* 2010; 67: 365–375.
9. Honey CJ and Sporns O. Dynamical consequences of lesions in cortical networks. *Hum Brain Mapp* 2008; 29: 802–809.
10. Carter AR, Shulman GL and Corbetta M. Why use a connectivity-based approach to study stroke and recovery of function? *Neuroimage* 2012; 62: 2271–2280.
11. Carrera E and Tononi G. Diaschisis: past, present, future. *Brain* 2014; 137: 2408–2422.
12. Saposnik G, Guzik AK, Reeves M, *et al*. Stroke Prognostication using Age and NIH Stroke Scale SPAN-100. *Neurology* 2013; 80: 21–28.
13. Prabhakaran S, Zarahn E, Riley C, *et al*. Inter-individual variability in the capacity for motor recovery after ischemic stroke. *Neurorehabil Neural Repair* 2007; 22: 64–71.
14. He BJ, Snyder AZ, Vincent JL, *et al*. Breakdown of functional connectivity in frontoparietal networks underlies behavioral deficits in spatial neglect. *Neuron* 2007; 53: 905–918.
15. Wang L, Yu C, Chen H, *et al*. Dynamic functional reorganization of the motor execution network after stroke. *Brain* 2010; 133: 1224–1238.
16. Dahms C, Brodoehl S, Witte OW, *et al*. The importance of different learning stages for motor sequence learning after stroke. *Hum Brain Mapp* 2020; 41: 270–286.
17. Fugl-Meyer AR, Jääskö L, Leyman I, *et al*. The post-stroke hemiplegic patient. 1. A method for evaluation of physical performance. *Scand J Rehabil Med* 1974; 7: 13–31.
18. Chai XJ, Castañón AN, Öngür D, *et al*. Anticorrelations in resting state networks without global signal regression. *Neuroimage* 2012; 59: 1420–1428.
19. Boes AD, Prasad S, Liu H, *et al*. Network localization of neurological symptoms from focal brain lesions. *Brain* 2015; 138: 3061–3075.
20. Tzourio-Mazoyer N, Landeau B, Papathanassiou D, *et al*. Automated anatomical labeling of activations in SPM using a macroscopic anatomical parcellation of the MNI MRI single-subject brain. *Neuroimage* 2002; 15: 273–289.
21. Laganiere S, Boes AD and Fox MD. Network localization of hemichorea-hemiballismus. *Neurology* 2016; 86: 2187–2195.
22. Beckmann CF, DeLuca M, Devlin JT, *et al*. Investigations into resting-state connectivity using independent component analysis. *Philos Trans R Soc Lond B Biol Sci* 2005; 360: 1001–1013.
23. Ovadia-Caro S, Villringer K, Fiebach J, *et al*. Longitudinal effects of lesions on functional networks after stroke. *J Cereb Blood Flow Metab* 2013; 33: 1279–1285.
24. Thijs VN, Lansberg MG, Beaulieu C, *et al*. Is early ischemic lesion volume on diffusion-weighted imaging an independent predictor of stroke outcome? A multivariable analysis. *Stroke* 2000; 31: 2597–2602.
25. Bagg S, Pombo AP and Hopman W. Effect of age on functional outcomes after stroke rehabilitation. *Stroke* 2002; 33: 179–185.
26. Schiemanck S, Post M, Kwakkel G, *et al*. Ischemic lesion volume correlates with long-term functional outcome and quality of life of middle cerebral artery stroke survivors. *Restor Neurol Neurosci* 2005; 23: 257–263.
27. Schiemanck S, Post M, Witkamp TD, *et al*. Relationship between ischemic lesion volume and functional status in the 2nd week after middle cerebral artery stroke. *Neurorehabil Neural Repair* 2005; 19: 133–138.

28. Stinear CM and Ward NS. How useful is imaging in predicting outcomes in stroke rehabilitation? *Int J Stroke* 2013; 8: 33–37.

29. Mazerolle EL, Beyea SD, Gawryluk JR, *et al*. Confirming white matter fMRI activation in the corpus callosum: co-localization with DTI tractography. *Neuroimage* 2010; 50: 616–621.

30. Gawryluk JR, Mazerolle EL, Brewer KD, *et al*. Investigation of fMRI activation in the internal capsule. *BMC Neurosc* 2011; 12: 56.

31. Fabri M and Polonara G. Functional topography of human corpus callosum: an FMRI mapping study. *Neural Plast* 2013; 2013.

32. Mazerolle EL, Gawryluk JR, Dillen KN, *et al*. Sensitivity to white matter fMRI activation Increases with field strength. *PLoS One* 2013; 8: e58130.

33. Gawryluk JR, Mazerolle EL and D'Arcy RC. Does functional MRI detect activation in white matter? A review of emerging evidence, issues, and future directions. *Front Neurosci* 2014; 8: 239.

34. Fox MD, Buckner RL, Liu H, *et al*. Resting-state networks link invasive and noninvasive brain stimulation across diverse psychiatric and neurological diseases. *Proc Natl Acad Sci USA* 2014; 111: E4367–E4375.

35. Bigourdan A, Munsch F, Coupé P, *et al*. Early fiber number ratio is a surrogate of corticospinal tract integrity and predicts motor recovery after stroke. *Stroke* 2016; 47: 1053–1059.

36. Engström M, Karlsson T and Landtblom A-M. Reduced thalamic and pontine connectivity in Kleine–Levin syndrome. *Front Neurol* 2014; 5: 42.

37. Brooks JC, Faull OK, Pattinson KT, *et al*. Physiological noise in brainstem FMRI. *Front Hum Neurosci* 2013; 7.

38. Harvey AK, Pattinson KT, Brooks JC, *et al*. Brainstem functional magnetic resonance imaging: disentangling signal from physiological noise. *Journal of Magn Reson Imaging* 2008; 28: 1337–1344.

39. Cramer SC. Repairing the human brain after stroke: I. Mechanisms of spontaneous recovery. *Ann Neurol* 2008; 63: 272–287.